Carbon rod of zinc-carbon primary battery waste as a substrate for CdS and TiO2 photocatalyst layer_Journal of Environmental Chemical Engineering_2017, 5, 2251

ORIGINALITY REPORT

16%	8%	13%	5%
SIMILARITY INDEX	INTERNET SOURCES	PUBLICATIONS	STUDENT PAPERS

PRIMARY SOURCES

1	Li, Qin, Xin Li, S. Wageh, Ahmed. A. Al-Ghamdi, and Jiaguo Yu. "CdS/Graphene Nanocomposite Photocatalysts", Advanced Energy Materials, 2015. Publication	2%
2	Rahmawati, Fitria; Wulandari, Rini; Murni, Irvina M. and Moedjijono, M.. "The Optical Properties and Photo catalytic Activity of ZnS-TiO_2/Graphite Under Ultra Violet and Visible Light Radiation", Bulletin of Chemical Reaction Engineering & Catalysis, 2015. Publication	1%
3	orca.cf.ac.uk Internet Source	1%
4	ejournal.undip.ac.id Internet Source	1%
5	umconference.um.edu.my Internet Source	1%

Digital Receipt

This receipt acknowledges that Turnitin received your paper. Below you will find the receipt information regarding your submission.

The first page of your submissions is displayed below.

Submission author:	Leny Yuliati
Assignment title:	Workshop Plagiarisme UMC
Submission title:	Carbon rod of zinc-carbon primary…
File name:	Journal_of_Environmental_Chemic…
File size:	1.3M
Page count:	8
Word count:	5,771
Character count:	28,774
Submission date:	17-Jan-2018 09:34PM (UTC+0700)
Submission ID:	903580637

Journal of Environmental Chemical Engineering 5 (2017) 2251–2258

Contents lists available at ScienceDirect

Journal of Environmental Chemical Engineering

journal homepage: www.elsevier.com/locate/jece

Carbon rod of zinc-carbon primary battery waste as a substrate for CdS and TiO_2 photocatalyst layer for visible light driven photocatalytic hydrogen production

Fitria Rahmawati[a,*], Leny Yuliati[b,c], Imam S. Alaih[a], Fatmawati R. Putri[a]

[a] Research Group of Solid State & Catalysis, Chemistry Department, Sebelas Maret University, Jl. Ir. Sutami 36 A, Kentingan, Surakarta 57126, Indonesia
[b] Ma Chung Research Center for Photosynthetic Pigments, Universitas Ma Chung, Villa Puncak Tidar N-01, Malang 65151, Indonesia
[c] Center for Sustainable Nanomaterials, Ibnu Sina Institute for Scientific and Industrial Research, Universiti Teknologi Malaysia, 81310 UTM Johor Bahru, Johor, Malaysia

ARTICLE INFO

Keywords:
Photocatalytic activity
CdS
TiO_2
Carbon rod waste
Photocatalytic hydrogen production

ABSTRACT

In this research, carbon rod as a solid waste of primary Zinc-Carbon batteries was used as a substrate for CdS and TiO_2 film. The film was deposited by chemical bath deposition with surfactant molecules as linker agent to promote the connection between the semiconductor film and the substrate. Material characterization was conducted to understand the phases content, its surface morphology, the quantum yield (QY) as measured through isopropanol degradation, and then their activity as a photocatalyst for visible light driven photocatalytic hydrogen production. XRD analysis found that the carbon rod waste is a mechanical mixture of amorphous carbon, represented by width broad peak lying between 22 and 25° and graphitic carbon, represented by a strong (002) peak at 26.3° and also a (001) peak at 42.2°. The result shows that CdS/Carbon (CdS/C) has higher photocatalytic activity than the TiO_2/Carbon (TiO_2/C) with the quantum yield value at 380 nm of a photon is 1.651×10^{-2}. Meanwhile, TiO_2/C provide the value of 1.495×10^{-4}. The QY value of CdS/C also higher than TiO_2/C at 450 nm of the light source. The H_2 production which was conducted with CdS/C performs 1.67 times higher than the production with TiO_2/C as a photocatalyst, i.e., 0.369 μmol s^{-1} g^{-1}. Meanwhile, the H_2 production rate with TiO_2/C is 0.222 μmol s^{-1} g^{-1}.

1. Introduction

Photocatalytic hydrogen production has received attention due to H_2 is a clean and renewable energy resource [1]. Some different mixed metal oxide semiconductors have been studied as the photocatalyst for hydrogen production [2–5], such as TiO_2 [6–9], $SrTiO_3$ [10], ZrO_2 [11], Ta_2O_5 [12] and WO_3 [13]. Among of them, titanium dioxide is still the most suitable in consideration of its activity, chemical inertness, low cost and non-toxicity [14,15]. Meanwhile, Cadmium sulfide is an II–VI group of semiconductor that has a wide band gap energy of 2.4 eV. The CdS has been used as an efficient material for solar cell due to its activity under visible light. CdS is a low band-gap semiconductor, that does act as photocatalysts for hydrogen production in aqueous media [16,17]. A CdS based solid solution, i.e., $Cd_{0.5}Sn_{0.5}Zn_{0.5-0.5}S$, and $Cd_{0.1}Zn_{0.9}S$ are known to have a high photocatalytic activity for hydrogen production under visible light radiation [18]. However, the photocatalytic activity of pure CdS semiconductor material still face some problems such as the adsorption ability of CdS toward the reactant particles, poor photostability, and serious aggregation with each other. The aggregation could reduce their surface area and increase the recombination rate of photogenerated charge carriers, thus leading to a decreased photoactivity [19].

A significant potential of carbonaceous materials according to its absorptivity character is a promising way to overcome the low absorption ability of CdS and TiO_2. It is known that the absorptivity of fullerene attributed to increasing catalytic activity of TiO_2 [20]. Graphene quantum dots as one of the carbonaceous materials known to has the ability on electron transfer reagent anchored on TiO_2 by in situ photo-assisted strategies, and it enhanced photocatalytic H_2 evolution activity in methanol aqueous solution without the noble metal co-catalyst [21]. An ultrafast transfer of photoexcited electrons from CdS to graphene sheet could significantly decrease the recombination rate of the photoexcited electrons and holes in CdS photocatalyst [19]. Graphene also is known as a good support for anchoring well-dispersed CdS, and it efficiently suppresses the aggregation and overgrowth of CdS [19]. Other carbonaceous material, such as graphite oxide also

* Corresponding author.
E-mail addresses: fitria@mipa.uns.ac.id, rahmawatifitria1@gmail.com (F. Rahmawati).

http://dx.doi.org/10.1016/j.jece.2017.04.032
Received 15 December 2016; Received in revised form 15 April 2017; Accepted 19 April 2017
Available online 21 April 2017
2213-3437/ © 2017 Elsevier Ltd. All rights reserved.

Carbon rod of zinc-carbon primary battery waste as a substrate for CdS and TiO2 photocatalyst layer_Journal of Environmental Chemical Engineering_2017, 5, 2251

by Leny Yuliati

Submission date: 17-Jan-2018 09:34PM (UTC+0700)
Submission ID: 903580637
File name: Journal_of_Environmental_Chemical_Engineering_2017,_5,_2251.pdf (1.3M)
Word count: 5771
Character count: 28774

Journal of Environmental Chemical Engineering 5 (2017) 2251–2258

Contents lists available at ScienceDirect

Journal of Environmental Chemical Engineering

journal homepage: www.elsevier.com/locate/jece

Carbon rod of zinc-carbon primary battery waste as a substrate for CdS and TiO_2 photocatalyst layer for visible light driven photocatalytic hydrogen production

Fitria Rahmawati[a,*], Leny Yuliati[b,c], Imam S. Alaih[a], Fatmawati R. Putri[a]

[a] Research Group of Solid State & Catalysis, Chemistry Department, Sebelas Maret University, Jl. Ir. Sutami 36 A, Kentingan, Surakarta 57126, Indonesia
[b] Ma Chung Research Center for Photosynthetic Pigments, Universitas Ma Chung, Villa Puncak Tidar N-01, Malang 65151, Indonesia
[c] Center for Sustainable Nanomaterials, Ibnu Sina Institute for Scientific and Industrial Research, Universiti Teknologi Malaysia, 81310 UTM Johor Bahru, Johor, Malaysia

ARTICLE INFO

Keywords:
Photocatalytic activity
CdS
TiO_2
Carbon rod waste
Photocatalytic hydrogen production

ABSTRACT

In this research, carbon rod as a solid waste of primary Zinc-Carbon batteries was used as a substrate for CdS and TiO_2 film. The film was deposited by chemical bath deposition with surfactant molecules as linker agent to promote the connection between the semiconductor film and the substrate. Material characterization was conducted to understand the phases content, its surface morphology, the quantum yield (QY) as measured through isopropanol degradation, and then their activity as a photocatalyst for visible light driven photocatalytic hydrogen production. XRD analysis found that the carbon rod waste is a mechanical mixture of amorphous carbon, represented by width broad peak lying between 22 and 25° and graphitic carbon, represented by a strong (002) peak at 26.3° and also a (001) peak at 42.2°. The result shows that CdS/Carbon (CdS/C) has higher photocatalytic activity than the TiO_2/Carbon (TiO_2/C) with the quantum yield value at 380 nm of a photon is 1.651×10^{-3}. Meanwhile, TiO_2/C provide the value of 1.495×10^{-4}. The QY value of CdS/C also higher than TiO_2/C at 450 nm of the light source. The H_2 production which was conducted with CdS/C performs 1.67 times higher than the production with TiO_2/C as a photocatalyst, i.e., 0.369 μmol s^{-1} g^{-1}. Meanwhile, the H_2 production rate with TiO_2/C is 0.222 μmol s^{-1} g^{-1}.

1. Introduction

Photocatalytic hydrogen production has received attention due to H_2 is a clean and renewable energy resource [1]. Some different mixed metal oxide semiconductors have been studied as the photocatalyst for hydrogen production [2–5], such as TiO_2 [6–13], $SrTiO_3$ [10], ZrO_2 [11], Ta_2O_5 [12] and WO_3 [13]. Among of them, titanium dioxide is still the most suitable in consideration of its activity, chemical inertness, low cost and non-toxicity [14,15]. Meanwhile, Cadmium sulfide is an II–VI group of semiconductor that has a wide band gap energy of 2.4 eV. The CdS has been used as an efficient material for solar cell due to its activity under visible light. CdS is a low band-gap semiconductor, that does act as photocatalyst for hydrogen production in aqueous media [16,17]. A CdS based solid solution, i.e., $Cd_{0.1}Sn_xZn_{0.9-2x}S$, and $Cd_{0.1}Zn_{0.9}S$ are known to have a high photocatalytic activity for hydrogen production under visible light radiation [18]. However, the photocatalytic activity of pure CdS semiconductor material still face some problems such as the adsorption ability of CdS toward the reactant particles, poor photostability, and serious aggregation with each other. The aggregation could reduce their surface area and increase the recombination rate of photogenerated charge carriers, thus leading to a decreased photoactivity [19].

A significant potential of carbonaceous materials according to its absorptivity character is a promising way to overcome the low absorption ability of CdS and TiO_2. It is known that the absorptivity of fullerene attributed to increasing catalytic activity of TiO_2 [20]. Graphene quantum dots as one of the carbonaceous materials known to has the ability on electron transfer reagent anchored on TiO_2 by in situ photo-assisted strategies, and it enhanced photocatalytic H_2 evolution activity in methanol aqueous solution without the noble metal co-catalyst [21]. An ultrafast transfer of photoexcited electrons from CdS to graphene sheet could significantly decrease the recombination rate of the photoexcited electrons and holes in CdS photocatalyst [19]. Graphene also is known as a good support for anchoring well-dispersed CdS, and it efficiently suppresses the aggregation and overgrowth of CdS [19]. Other carbonaceous material, such as graphite oxide also

* Corresponding author.
E-mail addresses: fitria@mipa.uns.ac.id, rahmawatifitria1@gmail.com (F. Rahmawati).

http://dx.doi.org/10.1016/j.jece.2017.04.032
Received 15 December 2016; Received in revised form 15 April 2017; Accepted 19 April 2017
Available online 21 April 2017

provide a good photocatalytic activity when it was intercalated with TiO_2. The electron transfer between TiO_2 with graphite might inhibit recombination of the excited electrons-holes [22]. Composite of CdS with all carbon form nanocomposites such as C60, NT, RGO, and solvent-exfoliated graphene, exhibit a quite similar enhancement in the photoactivity over CdS alone if the interfacial contact between carbon and semiconductors in all samples is intimate [23]. Therefore, it has been proven by many researchers that there is a synergistic effect between carbon support and titanium dioxide layer [24]. However, fullerene C60, carbon nanotubes, RGO and also graphene are carbonaceous materials that required a specific method and equipment to synthesize. The production frequently involves the use of toxic chemicals and also the high cost of large-scale production.

In another side, solid waste batteries increase year by year due to high demand on the portable electronic devices. More than 80% of batteries sold in Europe are a primary battery, in which the large majority of primary batteries are alkaline and zinc carbon batteries [25]. Every year around 160,000 tons of consumer batteries enter the European Union [26]. Meanwhile, according to the Environmental Protection Agency (EPA), each year Americans throw away more than three billion batteries, it is comparable to 180,000 tons of batteries, in which more than 86,000 tons of these are single-use alkaline batteries [27]. Many of the components of these batteries could be recycled, avoiding the release of hazardous substances to the environment. These will contribute to the improvement of environment quality. Zinc-carbon battery is a primary or disposable battery in which a carbon rod is inserted into electrolyte mixture and serve as a cathode. The carbon rod is a good electronic conductor with inert properties. An effort to reuse those carbon rod waste became another reason to use it as a substrate in this research, instead of graphene or other well synthesized carbonaceous materials.

2. Methods

2.1. Preparation of carbon disc

The carbon disc that used in this research was prepared from carbon rod extracted from the waste of zinc-carbon primary battery (ABC battery, produced by ABC industry, Indonesia). The carbon rods were cleaned by dipped into ethanol then washed with distilled water and dried at 105 °C in the oven for 1 h. The carbon rod then being sliced into a disc with a thickness of 1 mm and the diameter is 0.8 cm. The discs were cleaned by dipped into ethanol and ultrasonicated for 15 min before then being dried at room and continued with heating at 105 °C to remove humidity. The discs were then kept in a desiccator at room temperature and were weighed gravimetrically until the weight value difference was less than 0.02 mg.

2.2. Preparation of CdS/Carbon (CdS/C)

A 500 mL CdS solution was prepared from 0.1386 g of $CdSO_4$, 0.1013 g thiourea as precursors and $(NH_4)_2SO_4$ as a complexing agent. The ammonium salt was added to the solution and serves as a buffer. In this solution, the solvent is deionized water. The carbon disc was dipped into the CdS solution. Each tablet was dipped four times for 15 min for each dipping and under 70 °C condition, as it was optimized by our previous research [28]. The prepared CdS/C discs were also gravimetrically weighed as it was done for carbon disc.

2.3. Preparation of TiO_2/Carbon (TiO_2/C)

Meanwhile, TiO_2/C was also prepared by dipping the carbon disc into the synthesis solution that consists of 1.1 g $TiCl_4$ in a 100 mL of 1 M HCl and added with 0.583 g of CTAB. The process was conducting for four days under 60 °C. The green prepared discs were then cleaned and heated at 450 °C for 4 h. The prepared TiO_2/C were then gravimetrically weighed as it was done for carbon disc.

2.4. Material characterization and photocatalytic activity test

The prepared materials then were analyzed by X-ray diffraction (Shimadzu, Japan), a high-resolution UV–vis Spectrophotometer (UV 1700 Pharmaspec, Shimadzu, Japan) for diffuse-reflection analysis, and continued to Tauc plots analysis to determine their band gap energy.

Quantum yield (QY) of the prepared materials was measured as their activity on isopropanol degradation. A photocatalyst tablet with a diameter of 0.8 cm was into 4 mL of 2.5 M isopropanol solution in a cuvette, and then the cuvette was installed in the sample holder of UV–vis spectrophotometer (single-beam UV–vis mini 1240 spectrophotometer, Kasugawa, Shimazu, Japan). The cuvette is a quartz box, which is usually used for UV–vis spectrophotometer analysis. The width of the cuvette is 1.2 cm, length of 1.2 cm, and a tall of 4.5 cm. The volume of isopropanol solution was 40 mL, therefore due to a small volume and homogeneous phase of isopropanol, in this research, the degradation was conducted without stirring. After isopropanol solution had poured into the cuvette, then the spectrophotometer was tuned into the photometric menu, and the sample was irradiated by UV (380 nm of wavelength) and visible wavelength (450 nm and 517 nm for CdS/C). Radiation was conducted for 90 min, and the absorbance data was recorded in every 30 min. The QY value was calculated based on Eq. (1) [29].

$$QY = \frac{N_{mol}\,(mol.\ s^{-1})}{N_{photon}\,(molEinstein.\ s^{-1})} \quad (1)$$

N_{mol} is the number of isopropanol molecules transformed into a product, or the number of product formed during degradation. Meanwhile, N_{photon} is the number of photons absorbed by a photocatalyst material as measured by UV–vis diffuse reflectance spectroscopy.

To understand the contribution of the carbon disc to the degradation activity, this research also compared the catalytic performance of CdS film when the substrate is a glass (a quartz glass). Therefore, the CdS photocatalyst was compared in the same form i.e., the CdS film.

2.5. Photocatalytic hydrogen production test

The photocatalytic test was conducted in a Pyrex flask equipped with water condenser to keep the temperature of the reaction. The ambient temperature was 25.5 °C (298.65 K), the reaction temperature was 31.0 °C (304.15 K), and the ambient pressure was 1003 mbar (0.9899 atm). The prepared catalyst tablets with a mass of 0.0633 g were poured into 50 mL 0.35 M Na_2SO_3 solution and 50 mL of 0.25 M Na_2S solution, and it was stirred during the reaction. Nitrogen gas was purged into the flask for 30 min before the reaction started. Meanwhile, a 500-W mercury lamp (UV wavelength) was used as a photon source for 5 h of radiation time. The produced gas then analyzed by Thermal Conductivity Detector-Gas Chromatography (TCD-GC) to ensure the presence of hydrogen gas and then the quantity was determined by the volumetric method. The injection of produced gas was conducted at every 1 h. The rate of hydrogen production (μmol s^{-1} g^{-1}) was calculated for each catalyst to understanding the photocatalytic activity on H_2 production.

3. Result and discussion

Morphological analysis by Scanning Electron Microscope (SEM, JEOL JSM-6510, Germany) resulted in images as described in Fig. 1. The carbon disc shows a rough and non-homogeneous surface morphology (Fig. 1(a)). However, it became smooth and more homogenous after CdS deposition, as well as after TiO_2 deposition. CdS were deposited as flakes (Fig. 1(b) insert). Meanwhile, TiO_2 was deposited as small spheres with the size of less than 200 μm.

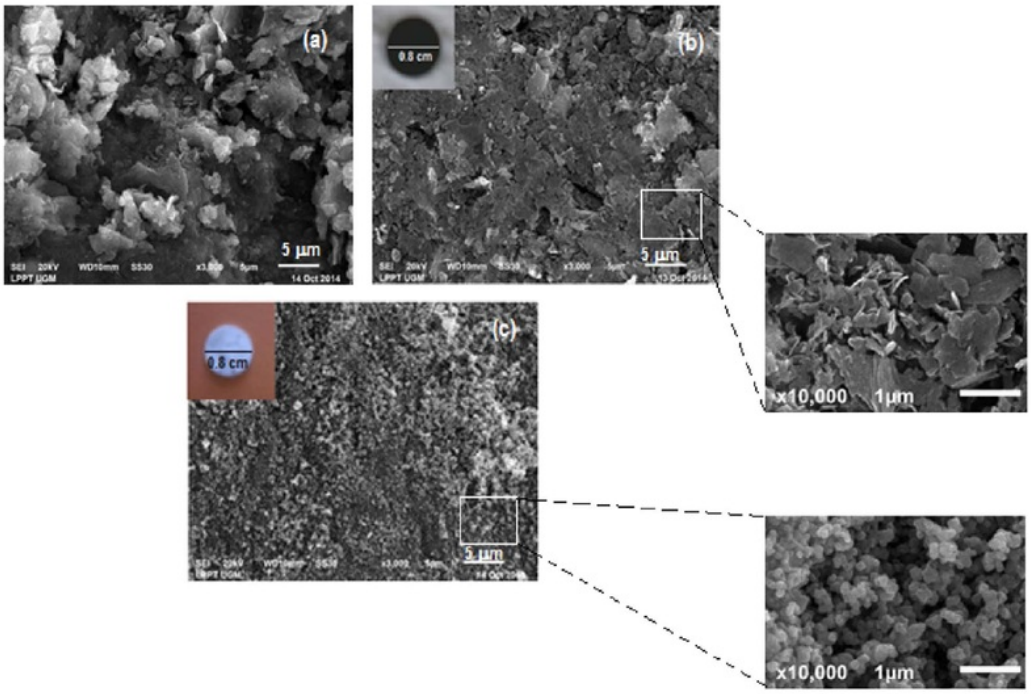

Fig. 1. SEM images of (a) graphite and (b) CdS/Graphite with CdS/Graphite photograph and the image at 10,000 magnification are inserted and (c) TiO_2/Graphite with TiO_2/Graphite photograph and the image at 10,000 magnification are inserted.

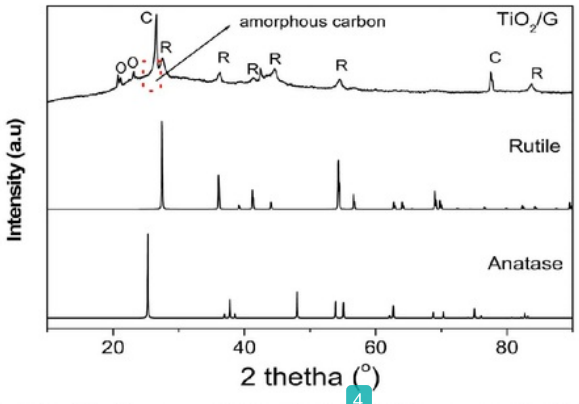

Fig. 2. The diffraction pattern of TiO_2/C and CdS/C. The TiO_2 layer consists of rutile, R, and anatase, A, phases. The O signs refer to CTAB peaks, C refers to carbon peaks.

X-ray diffraction pattern shows that TiO_2 present as rutile phase (Fig. 2), meanwhile a peak of graphitic carbon appears at 26.3°, as a strong and sharp peak of (002) plane [30]. A sharp peak at 44° also identified as graphitic carbon with (100) plane [31]. A peak at 2θ of 77.80° is identified as characteristic graphite peak based on the standard diffraction of graphite ICSD #28417. A broad peak with a width greater than 0.5°, that lying between 22 and 25° is considered as amorphous carbon [30]. Meanwhile, peaks at 2θ of 21.32° and 24.04° are CTAB peaks as confirmed by standard diffraction of JCPDS #48-2454 proof that the highest content of carbon rod waste is the carbon element supported by EDX analysis result as described in Fig. 3. The second dominant element is an oxygen atom that could be coming from graphitic oxide or other metal oxide or alkaline oxide as they were detected as trace elements (Fig. 3).

XRD pattern of CdS/C present peaks of CdS at 26.6° and a peak at 2θ of 55° as it is confirmed by the standard diffraction of CdS ICSD# 81925 (Fig. 4). The presence of CdS also shows by EDX analysis which detected at 0.02% (Fig. 5) and also shows by elemental mapping as described in Fig. 6, that confirm the presence of CdS on the carbon substrate. Data of weight change after CdS and TiO_2 deposition are listed in Table 1. Meanwhile, the EDX result of TiO_2/C shows an incorporation of TiO_2 on carbon substrate (Fig. 7).

Tauc plot of reflectance data is in Fig. 8. The Tauc plot direct transition of CdS/C (Fig. 8(a)), shows that the gap energy of CdS/C 2.39 eV. It is in agreement with the gap energy of CdS, i.e. 2.4 eV [16]. Meanwhile, the energy gap of TiO_2/C is 3.05 eV (Fig. 8(b)). It is in agreement with the previous research and also implies that in TiO_2/C, rutile phase has a dominant role in the photocatalytic process [29].

This research tried to ensure the contribution of carbon substrate into photo-catalytic activity of CdS film by conducting a photo-catalytic activity test to a CdS/glass and CdS/C with isopropanol molecules as the degradation target. The preparation and geometry of the CdS/glass itself were precisely similar to the CdS/C. The photo-catalytic test was conducted under UV (380 nm) and visible (450 nm) light. The results are in Fig. 9.

Fig. 9 shows that the degradation product is similar, shown by a new peak at 225–227 nm. The peak is indicated as a ketone functional group, as it was stated by Kumar (2006) [32] that ketone functional group shows an electronic transition of $\pi \rightarrow \pi^*$ at 180–195 nm. The peak will shift to longer wavelength in a more polar solvent. In this research, the solvent is water, a polar solvent, therefore the peaks are shifted to longer wavelength. When a UV wavelength of 380 nm irradiated the samples, the result shows that the degradation product is larger in the degradation system with CdS/glass as a photocatalyst, than in the system with CdS/C as a photocatalyst. It is known that silica has band gap energy, Eg of 8.7 ± 0.05 eV [33]. The value is high and requires high energy photon, at least ~142.5 nm to initiate an electronic transition. Therefore, when the UV light at 380 nm irradiated the CdS/glass, only CdS that undergo electron excitation, and the empty

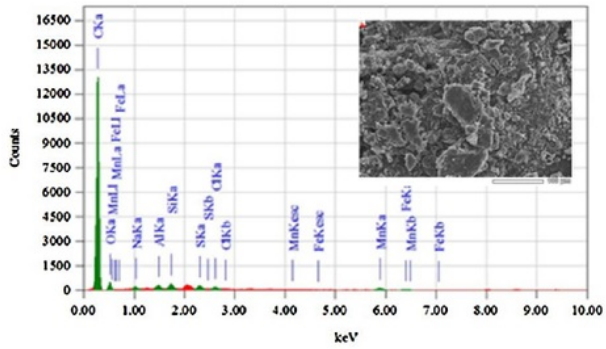

Element	C	O	Na	Al	Si	S	Cl	Mn	Fe	Total
KeV	0.277	0.525	1.041	1.486	1.739	2.307	2.621	5.894	6.398	
Mass%	85.22	11.90	0.20	0.33	0.50	0.42	0.25	0.86	0.31	100.00
Atom%	89.59	9.39	0.11	0.15	0.23	0.17	0.09	0.20	0.07	100.00

Fig. 3. EDX result on the carbon rod waste and the table of element content.

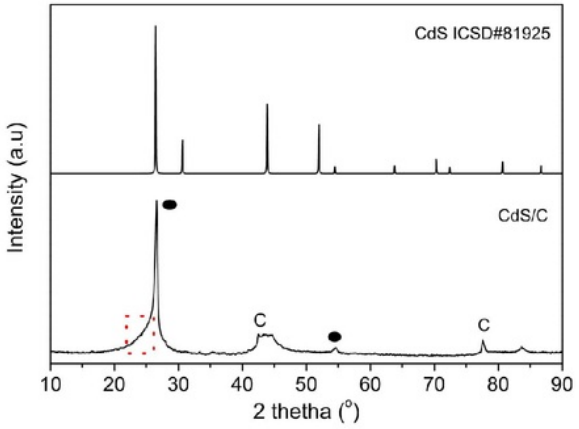

Fig. 4. XRD pattern of CdS/C compared to the standard diffraction of CdS ICSD #81925. The black circle is indicated as CdS peaks. Meanwhile C refers to carbon peaks.

a glass conduction band may serve as the electron receiver and reduce the possibility of electron-hole recombination. Meanwhile, the graphite substrate with amorphous carbon content inside is known to has a peak at around 4.0–5.0 eV (Fig. 8), which correlates to the light wavelength of 310–248 nm. Those peaks may contribute to the $\pi \rightarrow \pi^*$ transition. Graphite has an aromatic hydrocarbon compound containing benzene rings in its structure with the large delocalized itals around the benzene rings. Some $\pi \rightarrow \pi^*$ transitions are possible from the singlet ground state to the s et excited states. The optical absorption spectrum of graphite at visible range from 0 up to 5 eV originates from transition among π bands [34]. A calculation by Johnson and Dresselhaus [35] on the π bands in graphite, which were determined by McClure parameters along with the addition of in-plane neighbor's interactions, resulted in the allowed optical transitions near 5 eV. Interaction with CdS allows coupling mechanism that causes the absorption edge of the carbonaceous peak drop to the same point on the energy axis with the absorption edge of CdS peak (Fig. 8). Such interaction indicates that the carbonaceous substrate also active when the UV light used as a source, and it allows the conduction band of the strate were not available to be the electrons receiver and contribute to the reducing of electron-hole recombination.

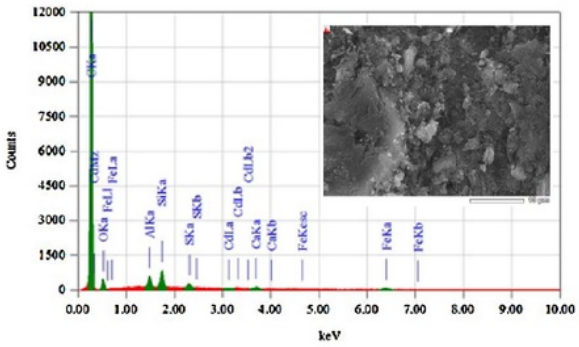

Element	C	O	Al	Si	S	Ca	Fe	Cd
KeV	0.277	0.525	1.486	1.739	2.307	3.690	6.398	3.132
Mass%	87.99	9.61	0.59	0.88	0.27	0.17	0.48	0.02
Atom%	91.56	7.51	0.27	0.39	0.10	0.05	0.11	0.00

Fig. 5. The EDX result of CdS/C and its elemental content.

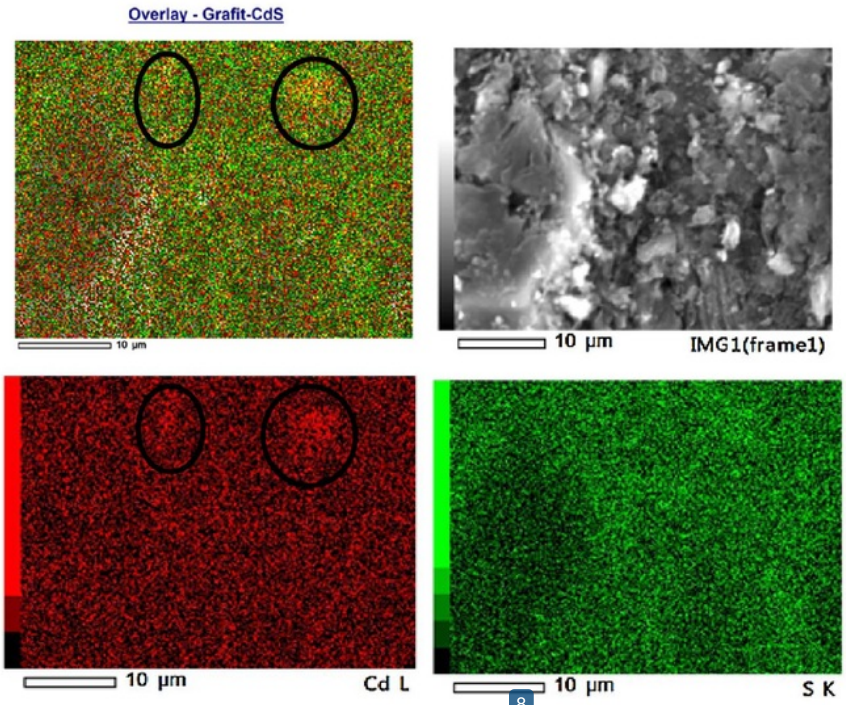

Fig. 6. The Cd and S mapping on CdS/C, black circle shows a high presence of Cd based on its red color. (For interpretation of the references to colour in this figure legend, the reader is referred to the web version of this article.)

Table 1
Weight of the initial carbon disc and the weight after the chemical bath deposition of CdS and TiO_2.

No.	Materials	The weight of C at initial (g)	Weight of CdS/C or TiO_2/C (g)	Weight of CdS or TiO_2 (g)
1.	CdS/C	0.109	0.122	0.013
		0.103	0.111	0.008
		0.087	0.091	0.004
			Average (g)	0.008 ± 0.003
2.	TiO_2/C	0.124	0.131	0.007
		0.118	0.127	0.009
		0.087	0.094	0.007
			Average (g)	0.008 ± 0.0005

A different result shows in Fig. 9(b) when the visible light of 450 nm was used as a photon source. In fact, the photon energy is insufficient to initiate an electronic excitation in the carbonaceous substrate, and allows the substrate to become a good electron sink to reduce the possibility of electron-hole recombination. Silica glass, whether the amorphous or crystalline phase is optically transparent to the optical energy of 0–5 eV [36]. It may allow large of photon past the CdS/glass without any photocatalytic mechanism to occur. Meanwhile, the carbonaceous substrate is not transparent optically and therefore can hold the photo to stay in the material and increase the possibility to be used by CdS to excite the electrons from valence band to conduction band. Therefore, it will be an advantage for carbonaceous substrate when the degradation proceeds with visible light as energy source. In addition, carbonaceous substrate is known as a good conductor that will allows them to be used in a photo-electro-assisted degradation system.

Photocatalytic activity test on isopropanol degradation with CdS/C and TiO_2/C as a catalyst also shows a new peak at 225–227 nm (Fig. 10). The absorbance at 225–227 nm is higher when CdS/C was used as photocatalyst than the absorbance when TiO_2/C was used under both radiation of 450 nm and 380 nm. In Fig. 10(a) the absorbance of the solution after being treated with CdS/C is over 1.0 when it was radiated by a high UV light energy. It is probably an indication of the photocatalyst layer exuviation which did not occur for TiO_2/C. The CdS exuviation is probably also occurred when the substrate is a silica glass, shown by a high absorbance over 1.0 (Fig. 9). It needs a further investigation regarding the quality of film attachment. However, this fact seems to do not affect the photocatalytic activity of the CdS/C, as it is found to be higher that TiO_2/C and the hydrogen production test also found the same conclusion. The activity is confirmed by the quantum yield, QY, values as listed in Table 2.

Under Ultraviolet radiation (380 nm), TiO_2/C has higher photon absorption in every second. However, the mole number of the product in every second (mole.s^{-1}) that is represented by absorbance value at 225–227 nm, is lower than the mole number of product in every second (mole s^{-1}) when the photodegradation proceed with CdS/C as the photocatalyst. Therefore, the QY value as calculated by Eq. (1) of TiO_2/C is lower than CdS/C at UV light radiation. The conduction band (CB) potential of CdS which is in a higher position of carbon allows migration of the excited electrons from the conduction band of CdS to the conduction band of carbon. The CB potential of CdS is −0.52 V (vs. NHE). Meanwhile, the CB potential of graphene as an allotrope of carbon is −0.11 to (−0.30) Volt (vs. NHE) [37]. Those CB potential position is leading thermodynamically to transfer photogenerated electrons from CdS to the carbon-based substrate. The intimate contact between CdS-carbon as well as the capability of carbon on capturing electrons further reduce the recombination of photogenerated electron-hole, and degradation reaction may proceed well. The lower bandgap of CdS, 2.39 eV, seem to increase the ability of an electron to excite from valence to conduction band, in comparison to the TiO_2 case, due to the higher band gap of TiO_2, 3.05 eV. Therefore, with the same substrate that can reduce recombination phenomena, the degradation seem to proceed faster and more efficient when CdS-Carbon as a couple than TiO_2-carbon as a couple.

This research provides Quantum Yield value as the parameter for

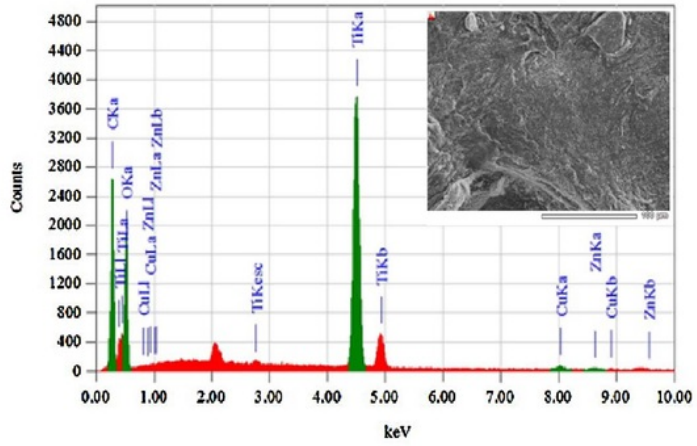

Element	C	O	Ti	Cu	Zn
KeV	0.277	0.525	4.508	8.040	8.630
Mass%	35.71	42.60	20.28	0.93	0.48
Atom%	48.89	43.79	6.96	0.24	0.12

Fig. 7. EDX result of TiO_2/C and its elemental content.

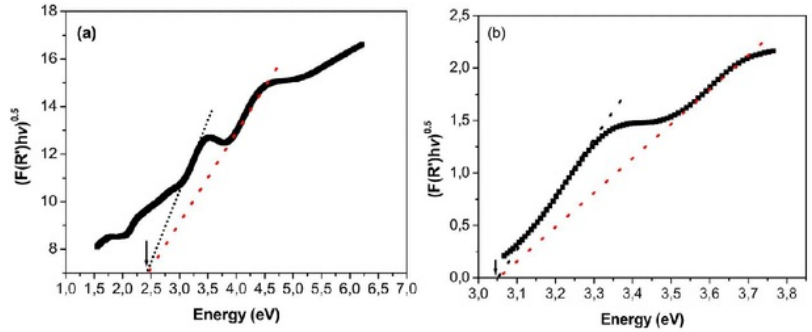

Fig. 8. Tauc plot of (a) CdS/C with Eg at 2.39 eV and (b) TiO_2/C with Eg of 3.05 eV.

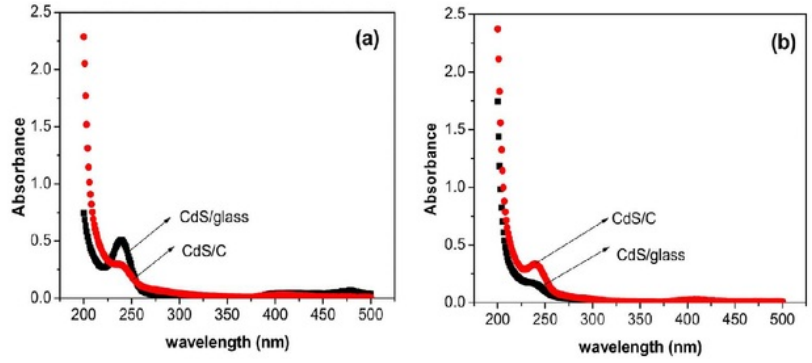

Fig. 9. The absorbance of the degraded isopropanol solution with CdS/C and CdS/glass after irradiation for 60 min with (a) UV light (380 nm) and (b) visible light (450 nm).

photocatalytic activity that confirms the production of degradation resulted in a second when the catalyst received photon in every second. This QY value is reliable for analysis of a fast photocatalytic degradation process, such as in this research in which the degradation was conducted for 90 min only. Other research in isopropanol degradation found that a further degradation occurs after the degradation proceeds for 5 h. The product of isopropanol degradation was propanone and acetaldehyde, and they undergo further degradation to CO_2. However, the CO_2 product was found only in a gas- solid system, in which the isopropanol to be degraded is in a gas phase. Further degradation to

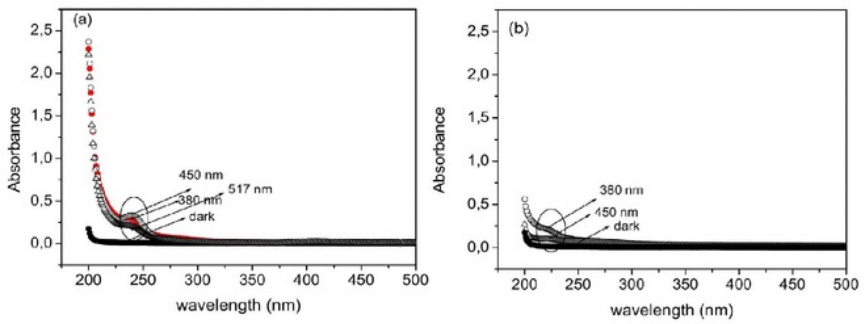

Fig. 10. UV–vis spectrum of isopropanol solution after degradation for 60 min with CdS/C (a) and with TiO_2/C (b) under various wavelength light.

Table 2
Quantum Yield of CdS/C and TiO_2/C at a various wavelength of radiation light for isopropanol degradation.

Materials	Wavelength (nm)	N_{mol} (mol/s)	N_{photon} (mol photon/s)	Quantum Yield	Relative QY
CdS/C	380	5.302×10^{-5}	3.21×10^{-2}	1.651×10^{-3}	11.05
	450	5.299×10^{-5}	5.89×10^{-2}	9.004×10^{-4}	6.03
	517	3.227×10^{-5}	5.89×10^{-2}	5.478×10^{-4}	3.67
TiO_2/C	380	3.303×10^{-5}	2.21×10^{-1}	1.495×10^{-4}	1.00
	450	0	4.23×10^{-4}	0	0

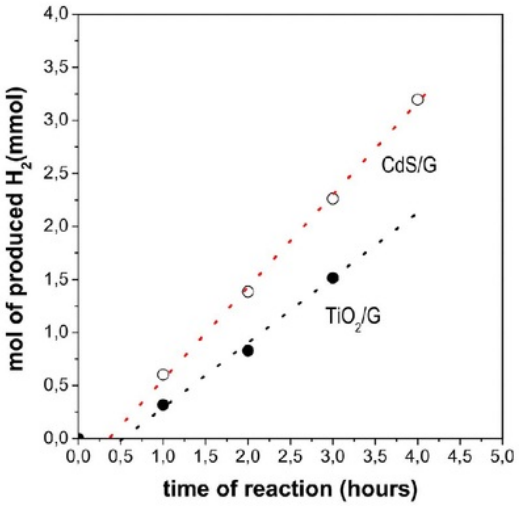

Fig. 11. The quantity of hydrogen production with CdS/C and TiO_2/C as photocatalyst.

CO_2 does not occur for the liquid-solid system [38].

A higher photocatalytic activity also occurred under visible light radiation. In which, it is clear that TiO_2 with high energy band gap, 3.05 eV, is not active in visible light because the energy of a photon is not sufficient to excite the electrons from valence band to conduction band. Even though, the photons were absorbed, as can be seen in Table 2. However, the photon is not active photo-catalytically. Instead of the TiO_2 layer, the carbon or graphitic carbon itself can absorb light and use it for $\pi \rightarrow \pi^*$ transition[35]. Therefore, the number of photon absorption might also serve as a contribution of the carbon substrate.

In term of photocatalytic activity for H_2 production, the hydrogen production rate with CdS/C is 1.67 times higher than the H_2 production rate with TiO_2/Graphite. The hydrogen production rate with CdS/C is 0.369 μmol s^{-1} g^{-1}. Meanwhile, the rate with TiO_2/C is 0.222 μmol s^{-1} g^{-1}. The curve of H_2 production with CdS/C and TiO_2/C are described in Fig. 11. The remarkable CdS performance also found when the nanotube TiO_2 (TiO_2NTs) was incorporated by CdS nanoparticle[23]. Meanwhile, photocatalytic hydrogen production with TiO_2 P25 powder produces rate of 3.04 μmol s^{-1} g^{-1} [1]. CdS can serve as a photosensitizer and the active photocatalyst itself. The mercury lamp that was used in this hydrogen production has a wavelength range between visible – ultraviolet light. The lines are 184.45 nm (UV-C), 253.7 (UV-C), 365.4 (UV-A), 404.7, 435.8, 546.1, and 578.2 (visible light). The CdS/C is known to active under ultraviolet and visible light (450 nm–517 nm) with QY values larger than TiO_2/C on that two kinds of light.

4. Conclusion

CdS/C has a higher photocatalytic activity that allows higher H_2 production than TiO_2/C whether under UV or visible light radiation. The QY value of CdS/C under UV light of 380 nm is 1.651×10^{-3}. It is 11.05 times of QY of TiO_2/C, i.e. 1.495×10^{-4}. Meanwhile, under visible light radiation, CdS/C shows photocatalytic activity with QY of 9.004×10^{-4}, in which TiO_2/C is inactive. The hydrogen production rate with CdS/C is 1.67 times higher than the H_2 production rate with TiO_2/C. The hydrogen production rate with CdS/C is 0.369 μmol s^{-1} g^{-1}. Meanwhile, the rate with TiO_2/C is 0.222 μmol s^{-1} g^{-1}.

Acknowledgement

Authors thank Sebelas Maret University, Indonesia for funding this research under Hibah Mandatory program 2016.

References

[1] G.L. Chiarello, E. Selli, L. Forni, Photocatalytic hydrogen production over flame spray pyrolysis-synthesised TiO_2 and Au/TiO_2, Appl. Catal. B: Environ. 84 (2008) 332–339.
[2] Z. Zou, J. Ye, K. Sayama, H. Arawa, Photocatalytic hydrogen and oxygen formation under visible light irradiation with M-doped InTaO4 (M = Mn, Fe, Co Ni, and Cu) photocatalysts, J. Photochem. Photobiol. A: Chem. 148 (1–3) (2002) 65–69.
[3] R. Abe, M. Higashi, K. Sayama, Y. Abe, H. Sugihara, Development of new photocatalytic water splitting into H_2 and O_2 using two different semiconductor photocatalysts and a shuttle redox mediator IO^{3-}/I^-, J. Phys. Chem. B 109 (33) (2005) 16052–16061, http://dx.doi.org/10.1021/jp052848l.
[4] W. Yao, J. Ye, Photocatalytic properties of a new photocatalyst $K_2Sr_{1.5}Ta_3O_{10}$, Chem. Phys. Lett. 435 (1–3) (2007) 96–99, http://dx.doi.org/10.1016/j.cplett.2006.12.047 2007.
[5] H. Kato, A. Kudo, Photocatalytic water splitting into H_2 and O_2 over various tantalate photocatalysts, Catal. Today 78 (1–4) (2003) 561–569, http://dx.doi.org/

10.1016/S0920-5861(02)00355-3.
[6] J. Nowotny, T. Bak, M.K. Nowotny, L.R. Sheppard, Titanium dioxide for solar-hydrogen I. Functional properties, Int. J. Hydrogen Energy 32 (14) (2007) 2609–2629, http://dx.doi.org/10.1016/j.ijhydene.2006.09.004.
[7] M. Hepel, Nanocrystalline structure and nanopore formation in modified thermal TiO2 films, Int. J. Hydrogen Energy 32 (14) (2007) 2693–2702, http://dx.doi.org/10.1016/j.ijhydene.2006.09.025.
[8] A.B. Murphy, P.R.F. Barnes, L.K. Randeniya, I.C. Plumb, I.E. Grey, M.D. Horne, The efficiency of solar water splitting using semiconductor electrodes, Int. J. Hydrogen Energy 31 (14) (2006) 1999–2017, http://dx.doi.org/10.1016/j.ijhydene.2006.01.014.
[9] S.S. Rayalu, N. Dubey, N.K. Labhsetwar, S. Kagne, S. Devotta, UV and visibly active photocatalysts for water splitting reaction, Int. J. Hydrogen Energy 32 (14) (2007) 2776–2783, http://dx.doi.org/10.1016/j.ijhydene.2007.03.028.
[10] M.S. Wrighton, A.B. Ellis, P.T. Wolczanski, D.L. Morse, H.B. Abrahamson, D.S. Ginley, Strontium titanate photoelectrodes. Efficient photoassisted electrolysis of water at zero applied potential, J. Am. Chem. Soc. 98 (10) (1976) 2774–2779, http://dx.doi.org/10.1021/ja00426a017.
[11] S.H. Liu, H.P. Wang, Photocatalytic generation of hydrogen on Zr-MCM-41, Int. J. Hydrogen Energy 27 (9) (2002) 859–862, http://dx.doi.org/10.1016/S0360-3199(01)00190-2.
[12] K. Sayama, H. Arakawa, Effect of Na2CO3 addition on the photocatalytic decomposition of liquid water over various semiconductor catalysis, J. Photochem. Photobiol. A Chem. 77 (2–3) (1994) 243–247, http://dx.doi.org/10.1016/1010-6030(94)80049-9.
[13] A. Hameed, M.A. Gondal, Z.H. Yamani, Effect of transition metal doping on photocatalytic activity of WO_3 for water splitting under laser illumination: role of 3d-orbitals, Catal. Commun. 5 (11) (2004) 715–719, http://dx.doi.org/10.1016/j.catcom.2004.09.002.
[14] M. Ni, M.K.H. Leung, D.Y.C. Leung, K. Sumathy, A review and recent developments in photocatalyticwater-splitting using TiO_2 for hydrogen production, Renew. Sustain. Energy Rev. 11 (2007) 401, http://dx.doi.org/10.1016/j.rser.2005.01.009.
[15] A. Fujishima, T.N. Rao, D.A. Tryk, Titanium dioxide photocatalysis, J. Photochem. Photobiol. C 1 (1) (2000) 1–21, http://dx.doi.org/10.1016/s1389-5567(00)00002-2.
[16] T. Dhandayuthapani, M. Girish, R. Sivakumar, C. Sanjeeviraja, R. Gopalakrishnan, Tuning the Morphology of Metastable MnS Films bySimple Chemical Bath Deposition Technique, App. Surf. Sci. 353 (2015) 449–458, http://dx.doi.org/10.1016/j.apsusc.2015.06.154.
[17] M. Ashokkumar, An overview of semiconductor particulate systems for photoproduction of hydrogen, Int. J. Hydrogen Energy 23 (1998) 427, http://dx.doi.org/10.1016/S0360-3199(97)00103-1.
[18] M. Sathish, R.P. Viswanath, Photocatalytic generation of hydrogen over mesoporous CdS nanoparticle: effect of particle size, noble metal, and support, Catal. Today 129 (2007) 421–427, http://dx.doi.org/10.1016/j.cattod.2006.12.008.
[19] M. Kimi, L. Yuliati, M. Shamsuddin, Photocatalytic hydrogen production under visible light over Cd0. 1SnxZn0. 9-2xS solid solution photocatalysts, Int. J. Hydrogen Energy 36 (2011) 9453–9461, http://dx.doi.org/10.1016/j.ijhydene.2011.05.044.
[20] J. Sabate, S. Cervera-March, R. Simarro, J. Gimenez, Photocatalytic production of hydrogen from sulfide and sulfite waste streams: a kinetic model for reactions occurring in illuminating suspensions of CdS, Chem. Eng. Sci. 45 (10) (1990) 3089–3096, http://dx.doi.org/10.1016/0009-2509(90)80055-J.
[21] E. Regulska, J. Karpinska, Investigation of photocatalytic activity of C60/TiO_2 nanocomposites produced by evaporation drying method, Pol. J. Environ. Stud. 23 (6) (2014) 2175–2182.
[22] X. Hao, Z. Jin, J. Xu, S. Min, G. Lu, Functionalization of TiO_2 with graphene quantum dots for efficient photocatalytic hydrogen evolution, Superlattices Microstruct. 94 (2016) 237–244.
[23] H. Yunqiu, W. Ruihua, W. Jingjing, X. Qinghong, Microstructure evolution of graphite intercalated by TiO_2 and its photocatalytic activity, J. Wuhan Univ. Technol. Mater. Sci. 24 (2) (2009) 223–228.
[24] X. Hao, Z. Jin, J. Xu, S. Min, G. Lu, Functionalization of TiO_2 with graphene quantum dots for efficient photocatalytic hydrogen evolution, Superlattices Microstruct. 94 (2016) 237–244. 2016.
[25] J. Lang, V. Majetka, Graphite/Titanium dioxide composite, Proceeding of NANOCON 2013, October 16–18, 2013, Brno, Czech Republic, European Union, 2013.
[26] www.epbaeurope-net/whatis.html, Accessed on 10 October, 2016.
[27] http://ec.europa.eu/environment/waste, Accessed on 11 October, 2016.
[28] http://everyday-green.com/html/battery_statistic.html, Accessed on 10 October, 2016.
[29] F. Rahmawati, R. Wulandari, E. Nofaris, Mudjijono, Optical properties and photocatalytic activity of CdS-TiO_2/graphite composite, Sci. Eng. Compos. Mater. 24 (2) (2017) 253–260.
[30] P.L. Walker, J.F. Rakszamski, A.F. Annington, X-ray diffraction studies of a graphitized carbon, ASTM Bull. 208 (1955) 52–54.
[31] C.H. Kim, T. Oh, Graphitic mesostructured carbon from an aliphatic hydrocarbon precursor, Bull. Korean Chem. Soc. 30 (9) (2009) 1978–1980.
[32] S. Kumar, Organic Chemistry: Spectroscopy of Organic Compounds, Department of Chemistry, Guru Nanak Dev University, Amritsar, 2006, pp. 1–36.
[33] J.D. Jorgensen, Compression mechanisms in α-quartz structures—SiO_2 and GeO_2, J. Appl. Phys. 49 (11) (1978) 5473–5478.
[34] P.E. Trevisanutto, M. Holzmann, M. Côté, V.1 Olevano, *Ab initio* high-energy excitonic effects in graphite and graphene, Phys. Rev. B 81 (12) (2010) 121405.
[35] L.G. Johnson, G. Dresselhaus, Optical properties of graphite, Phys. Rev. B 7 (1973) 2275–2285.
[36] S.S. Nekrashevic, V.A. Gritsenko, Electronic structure of silicon dioxide (A review), Phys. Solid State 56 (2) (2013) 207–222.
[37] X. Li, S. Wageh, A.A. Al-Ghamdi, CdS/Graphene nanocomposite photocatalysts, Adv. Energy. Mater 1500010 (2015) 1–28.
[38] G. Marcì, E. García-López, G. Mele, L. Palmisano, G. Dyrda, R. Slota, Comparison of the photocatalytic degradation of 2-propanol in gas-solid and liquid-solid systems by using TiO_2-$LnPc_2$ hybrid powders, Catal. Today 143 (2009) 203–210.